Assessment of the suitability of gravel wash mud as raw material for the synthesis of an alkali-activated binder

Vishojit Bahadur Thapa, Danièle Waldmann, Jean-Frank Wagner, André Lecomte

Vishojit Bahadur Thapa, Laboratory of Solid Structures, University of Luxembourg.

Danièle Waldmann, Laboratory of Solid Structures, University of Luxembourg, Tel.: +352 46 66 44 5279,

E-mail: daniele.waldmann@uni.lu.

Jean-Frank Wagner, Department of Geology, University of Trier.

André Lecomte, Institut Jean Lamour, University of Lorraine, Nancy, France.

Abstract **–** Gravel wash mud (GWM), a waste product from gravel mining was dried and processed into a fine powder to be activated by different concentrations of sodium hydroxide (NaOH) solutions for the synthesis of an alkali-activated binder. The GWM powders were thermally treated at five different calcination temperatures 550, 650, 750, 850 and 950°C. The characterisation of the raw material comprises the particle size distribution (PSD) by laser granulometry, the chemical and mineralogical composition by X-ray fluorescence and X-ray diffraction analysis respectively, and simultaneous thermal analysis. The performance of the alkali-activated binders were examined using compression strength tests and the microstructure was observed using scanning electron microscopy (SEM). The GWM was classified as an aluminosilicate raw material with kaolinite and illite as main clay minerals. Furthermore, a mean particle size around 6.50 μm was determined for the uncalcined and calcined GWM powders. The SEM images of the developed binders showed the formation of a compact microstructure, however, relatively low strengths were achieved. This preliminary study highlights an example of an aluminosilicate prime material, which shows very promising chemical and mineralogical characteristics, but its suitability for alkaline activation without further additives was not confirmed as far as performance-based criteria are considered.

Keywords **-** Gravel wash mud, thermally activated clays, alkali-activated binder, illite, kaolinite

1 INTRODUCTION

Today's trend of revalorising waste products or industrial by-products to reduce the use of Ordinary Portland Cement (OPC) in building or road constructions has become an ambitious goal and a key objective of current political strategies, industries and research institutions (Friedlingstein et al., 2014; Garcia-Gusano et al., 2015; Liu et al., 2015). Concrete, mainly based on OPC, is stated as the second most used material in the world after water and its production generates up to 5% of the overall annual CO_2 emissions worldwide. One of the main factors responsible for the unfavourable ecological performance of OPC is the high CO_2 emissions linked to the cement production processes like clinker burning including the chemical conversion of limestone ($CaCO_3$) into lime (CaO) and the emissions related to the fossil fuel combustion during cement production (Salas et al., 2016). Nevertheless, the current demand for cementitious binder is reaching record values each year and this trend is likely to increase. However, the incentive of developing sustainable and robust building concepts using alternative construction materials has become increasingly relevant. Therefore, there is a growing challenge in the research communities to develop new, durable and environmental friendly binders as an alternative to OPC binders (Shi et al., 2011).

The concepts of alkali-activated binders or geopolymer cements are intensively investigated and discussed as a very promising alternative to OPC. However, even if the concepts of alkali-activated materials and the geopolymer technology are researched since last mid-century, there are discrepancies and no overall accepted consensus considering the terminology of these materials. **Fig. 1** shows a short illustration of the general differences between alkali-activated binders and geopolymers in terms of characteristics of the raw materials, activating solutions and reaction mechanisms.

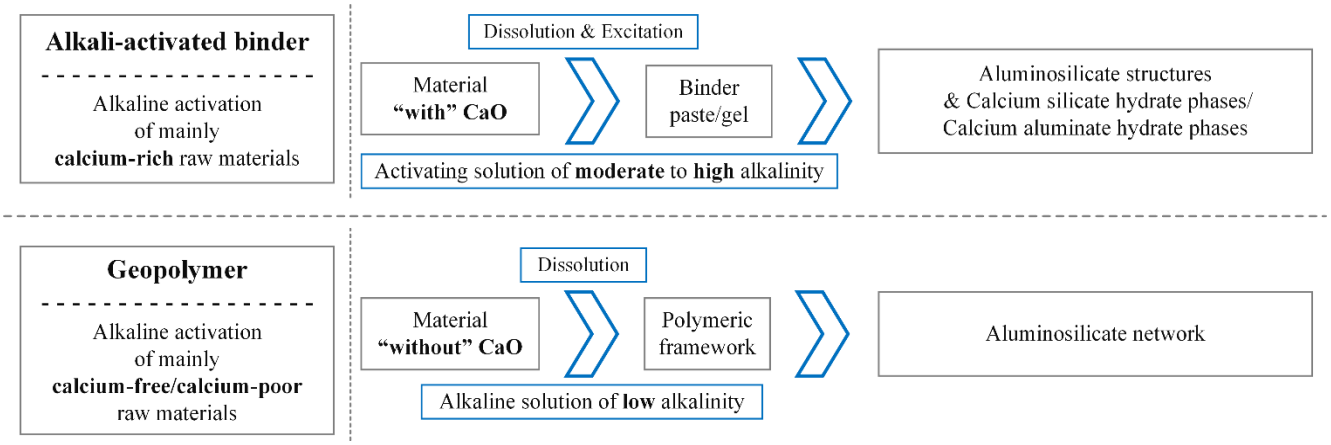

Fig. 1: Overview of the general reaction mechanisms of alkali-activated binder and geopolymer

Glukhovsky (1959) was the pioneer in this field of research as he extensively studied the presence of analcime phases, which are classified as zeolites, in the cements of ancient constructions and later developed binders made from aluminosilicates in reaction with alkaline industrial wastes, which he named "soil silicate concrete" and "soil cements". The early investigations on alkali-activated binders mainly focused on the activation of blast furnace slag, a by-product of the metallurgical industry. After, the next wave of interest raised after the results of Davidovits (1979, 1994), who developed and patented a novel binder (Davidovits and Sawyer, 1985; Heitsmann et al., 1987) which he named "geopolymer cement". The first geopolymer binder was a slag-based geopolymer cement, which consisted of metakaolin, blast furnace slag and alkali silicate. The main driver for the development of this technology is the lower environmental impact compared to OPC technology. Several authors have evaluated the CO_2 emissions related to the production of these binders and have stated significant reductions of up to 80% lower CO_2 emissions compared to cement production (Davidovits et al., 1990; Provis and Van Deventer, 2009). Further benefits over conventional concrete is the rapid strength gain while reaching the maximal strength at early hours and the development of a durable and compact microstructure (Davidovits, 1994). Moreover, higher thermal resistance, higher resistance to chemical attack, low permeability and better passivation of the steel reinforcement have been identified (Pacheco-Torgal et al., 2012; Aguirre-Guerrero et al., 2017). Finally, the production of alkali-activated binders or geopolymer cements provides a sustainable and viable alternative use for "waste" materials, which have to be very uneconomically disposed in landfills.

Subsequent studies have been carried out based on these original material concepts and various authors have contributed by their research to the understanding of the chemical mechanism and the development of alkaline binders (Glukhovsky, 1980; Shi et al., 1991; Roy et al., 1992; Wang et al., 1994; Wang and Scrivener, 1995; Wang et al., 1995; Phair and Van Deventer, 2001; Escalante-Garcia et al., 2003; Yunsheng et al., 2010; Le Saoût et al., 2011, Provis, 2014, 2017; Provis et al., 2015; Myers et al., 2017; Wianglor et al., 2017).

However, the application of these binders in construction elements has already become challenging as the price of these commercially available raw materials has risen over the last decades due to the high demand and the limited raw material availability, which is highly dependent on the primary industrial processes. Therefore, there is a trend to investigate on alternative prime materials to be revalorised for development of alkali-activated binders.

Sun et al. (2013) investigated on the synthesis of geopolymers out of waste ceramics, which were activated by alkali hydroxides and/or sodium/potassium silicate solutions. The maximum compressive strength for the synthesized geopolymer pastes measured after 28 days was 71.1 MPa and favourable thermodynamically stable properties in terms of compressive strength evolution after thermal exposures were observed. Pacheco-Torgal et al. (2007) investigated on an alternative to OPC using tungsten mine waste mud as prime material. The mineralogical analysis indicated the presence of muscovite and quartz minerals. After activation with a mix of sodium hydroxide and sodium silicate, different fine aggregates were added and the new binders showed very high strength at early ages. The compressive strengths for the different mixtures measured after 28 days ranged from about 60 to 75 MPa. Poowancum et al. (2015) developed a geopolymer binder using water-treatment-sludge and rice husk ash as raw material. The alkaline activator used was a mixture of sodium hydroxide and sodium silicate and the resulting maximal strengths were around 16 MPa for a rice husk content of 30%. Chen et al. (2009) studied the practicability of calcined sludge from a drainage basin of a water reservoir as a precursor for alkaline activation into an inorganic polymer. The raw material consisted of a sludge containing fractions of silts and smectite clays with high content of aluminosilicates (around 85%) and some impurities. The maximum compressive

strength measured after 28 days was 56.2 MPa using the raw material calcined at 850°C.

Ferone et al. (2013) examined the potential of two clay sediments from different reservoirs, Occhito and Sabetta, as raw material for the production of geopolymer binder. These sediments were subjected to different calcination treatments and the binder was synthesized by mixing the calcined aluminosilicates with 5 M NaOH solutions. After undergoing different curing conditions, the mechanical performance of the samples was examined. In general, a rapid strength development was observed and the maximal achieved compressive strength was around 10 MPa for the samples made of Sabetta sediments. Finally, the authors stated that the calcination temperature applied to the sediments plays a major role in the effectiveness of the geopolymerisation.

Molino et al. (2014) performed a similar series of experiments on calcined sediments from Occhito reservoir to synthesise binders using various concentrations of three different alkaline solutions, namely sodium hydroxide solution, sodium aluminate solution and potassium aluminate solution. The authors recommended for impure precursors with low content of alumina to use alumina-containing activating solutions as the samples activated with the sodium aluminate solution showed the best mechanical performance and achieved compression strengths up to 7 MPa.

Recently, Messina et al. (2017) conducted investigations on the production of precast building elements by the synthesis of geopolymer binders based on water potabilization sludge and clayey sediments, both considered as waste products from reservoir management. After calcination, different proportions of the raw materials were activated using a mixture of sodium silicate solution and a 14 M sodium hydroxide solution. The highest mechanical performance of the binders is stated around 23 MPa in compression strength and around 2 MPa in tensile splitting strength.

In general, further research on potential alternative raw materials could approve their adequacy for OPC replacement as a high compressive strength and low cost alkali-activated binder (Balek and Murat, 1996; Buchwald et al., 2009a, 2009b; Yunsheng et al., 2010; Bignozzi et al., 2013; Gartner and Hirao, 2015).

In this work, the suitability of a waste material, gravel wash mud (GWM), as raw material for the development of novel binders is examined by conducting different material characterisation techniques

and experimental tests. The main focus relies on finding the best parameters for the calcination of the GWM powders. An optimal calcination time and temperature range will be suggested after exposure to selected high temperatures ranging from 550°C to 950°C. The raw materials were characterised by simultaneous thermal analysis (thermogravimetric analysis and differential scanning calorimetry, TG-DSC), XRF and XRD. An optimal alkali-activated binder is selected based on mechanical testing and the evaluations based on SEM images. The findings of this study will enrich the investigations on alkali-activation of alternative raw materials to revalorise waste products economically and environmentally.

2 EXPERIMENTAL PROCEDURE

2.1 Materials

The prime material for this study, gravel wash mud (GWM), originates from Folschette (Rambrouch, Luxembourg) and consists of wet deposits, which occur during gravel extraction, more precisely during the washing of sand and gravel aggregates. The reddish brown mud is quite homogeneous and has a very plastic consistency. The raw material was extracted from a storage basin and provided by Carrières Feidt S.A., the operating company of the quarry. The geological analysis of the extraction site reveals that the rock strata mainly consists of red sandstone (ger. Buntsandstein) in form of conglomeratic deposits of sand and silt layers (Wagner, 1989; Lucius, 1948, 1950).

The GWM was dried at 105°C in a laboratory oven until reaching a constancy of mass (± 2 days) and the dried prime material was ground into a fine powder. In the following process, the powder was calcined for 1h at different temperatures 550°C, 650°C, 750°C, 850°C and 950°C (heating rate of about 5°C/min) in a laboratory chamber furnace with radiation heating (Nabertherm, Model N41/H).

The sand aggregates used were CEN-standard sands according to EN 196-1. The standard sand has a characteristic grain size distribution with particle sizes ranging between 80 µm and 2 mm.

The hydroxide (NaOH) solutions were prepared by dissolving commercially available NaOH pellets (≥ 99% purity) in different portions of distilled water to obtain NaOH solutions of different molar concentrations (8M, 10M and 14M). As the dissolution process of NaOH is an exothermic reaction, the solutions were let to cool down in sealed bottles to avoid evaporation and the capture of carbon dioxide

(CO_2) from air to form sodium carbonate. The bottles were stored for 24 h at room temperature before usage.

2.2 Synthesis of the alkali-activated binder and mixing proportions

Two large series of alkali-activated binders were prepared (**Fig. 2**). The first series consists of binders, which were prepared by mixing different calcined GWM powders with three concentrations of NaOH solutions, 8 M, 10 M and 14 M. The second series of mixtures comprises the same mixing materials with further addition of standard CEN sand at mass proportions of 3:1 to the calcined GWM powders. The incorporation of aggregates allows to analyse the coverage of the grains by the binder and to verify the formation of a more compact microstructure with higher mechanical performance. The liquid/solid (L/S) ratio represents the relation between the contents by mass of the alkaline solution and the solid constituents (GWM powders and sand). This ratio was kept constant for both series of mixtures at 0.7, respectively 0.8 (except 0.9 for 14M with addition of sand). Finally, nine specimens from each mixture were prepared to have specimens for different curing times, 14 days, 28 days and 56 days (3 specimens for each curing time). In total, 270 specimens were prepared using the compositions and mixing proportions as listed in **Table 1**.

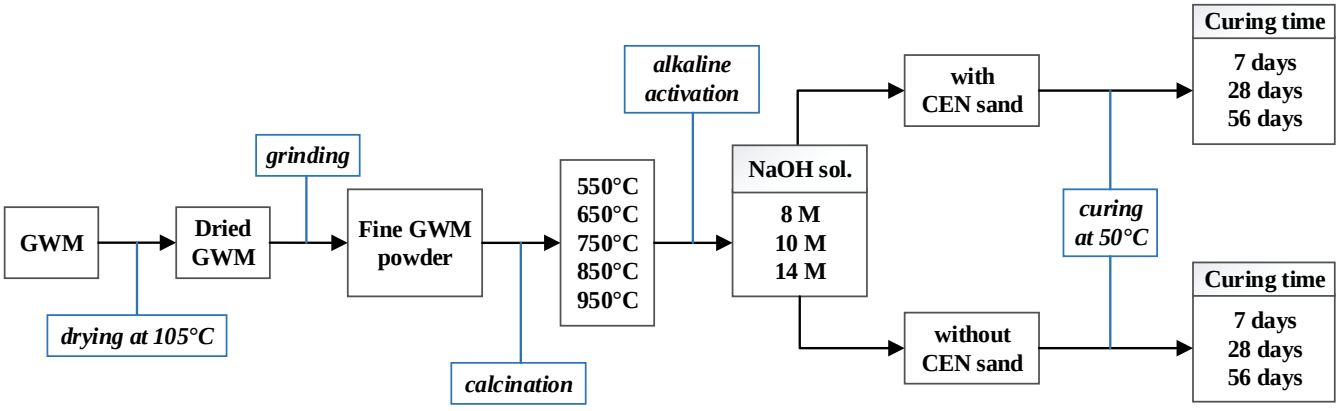

Fig. 2: Overview of the mixture composition of the alkali-activated binders

Sample ID	CT[1]	M[2]	L/S ratio[3]	S:G[4]	Sample ID	CT	M	L/S ratio	S:G
G_550_8		8 M			GS_550_8		8 M	0.8	
G_550_10	550°C	10 M			GS_550_10	550°C	10 M	0.8	
G_550_14		14 M			GS_550_14		14 M	0.9	
G_650_8		8 M			GS_650_8		8 M	0.8	
G_650_10	650°C	10 M			GS_650_10	650°C	10 M	0.8	
G_650_14		14 M			GS_650_14		14 M	0.9	
G_750_8		8 M			GS_750_8		8 M	0.8	
G_750_10	750°C	10 M	0.7	-	GS_750_10	750°C	10 M	0.8	3:1
G_750_14		14 M			GS_750_14		14 M	0.9	
G_850_8		8 M			GS_850_8		8 M	0.8	
G_850_10	850°C	10 M			GS_850_10	850°C	10 M	0.8	
G_850_14		14 M			GS_850_14		14 M	0.9	
G_950_8		8 M			GS_950_8	950°C	8 M	0.8	
G_950_10	950°C	10 M			GS_950_10		10 M	0.8	
G_950_14		14 M			GS_950_14		14 M	0.9	

[1] CT - Calcination temperature
[2] M - Molarity of activating solution
[3] L/S - Liquid to solid (mass) ratio
[4] S:G - Sand to GWM (mass) ratio

Further information:
- Designation principle: G(S)_CT_M with "G" for GWM & "GS" for GWM with sand
- 3 specimens per curing time (14 days, 28 days and 56 days) were prepared for each mixture

Table 1: Mixing proportions of all investigated alkali-activated binders

The mixtures without additional aggregates were prepared by adding the calcined GWM powder in a mixing bowl and by mechanically mixing the powders at a speed of 125 rpm for 90s with gradual addition of the alkaline solution. Subsequently, the mixture was mixed at a speed of 250 rpm for 90s until a good processable compound has formed. The mixing procedure of the binders with additional aggregates consists of primarily preparing the binder (GWM and alkaline solution; at 125 rpm for 90s). Afterwards, the CEN-standard sand was gradually added and mechanically intermixed at a mixing speed of 125 rpm for 60s and later at 250 rpm for 90s until stoppage.

The prepared binder compounds were poured in prismatic moulds (40x40x160 mm^3) and vibrated for 7 seconds. Then, the moulds were covered using plastic plates of 5 mm thickness and additionally wrapped in cellophane foil to prevent desiccation of the samples and rapid loss of moisture. The mixtures were let to cure inside the moulds in a ventilated oven at 50°C. After demoulding, the specimens were sealed in cellophane foil and stored at 50°C until 24 hours before the compression strength test.

3 APPLIED CHARACTERISATION METHODS AND RESULTS

3.1 Physical and chemical characterization of the GWM powders

The PSD of the powders were evaluated by laser granulometry using a modular analysis system (HELOS and RODOS from Sympatec GmbH). Laser granulometry follows the methods of laser diffraction based on Fraunhofer diffraction physics (Cowley, 1995). This measurement unit is applicable on all kind of dry powders. The particle size distribution of the GWM powders is shown in **Fig. 3**. The particle size mainly comprises within a range of 1 to 35 µm with a mean particle size (d50) around 6.50 µm, whereas, comparatively mean particle size of cement powder ranges around 10-12 µm. The PSD analysis of the GWM powders calcined at different temperatures resulted in a similar grain size distribution beside for the powders calcined at 850°C and 950°C, where a slight shift of the curves to coarser particle sizes was observed due to the clumping of the powders related to the effect of sintering of fine clay particles (Aramide, 2015).

The specific surface area of the powder samples, determined following the BET method (Brunauer et al., 1938), was at 14.5 m^2/g. Furthermore, the chemical composition of the GWM powder was determined using a wavelength dispersive X-ray fluorescence spectrometer (S4 Explorer from Bruker Corporation) with a flexible integrated auto sampler. The samples were prepared by pelletisation of a mix of loose GWM powder with wax in a ring using the pressed powder technique. The calcination parameters of the GWM powders were verified by the study of mineralogical phase transition and thermal analysis. The chemical composition of the GWM powder is listed in **Table 2**. The analysis of the chemical constitution verifies that the raw material mainly consists of aluminosilicate particles with primary chemical elements of SiO_2, Al_2O_3 and Fe_2O_3.

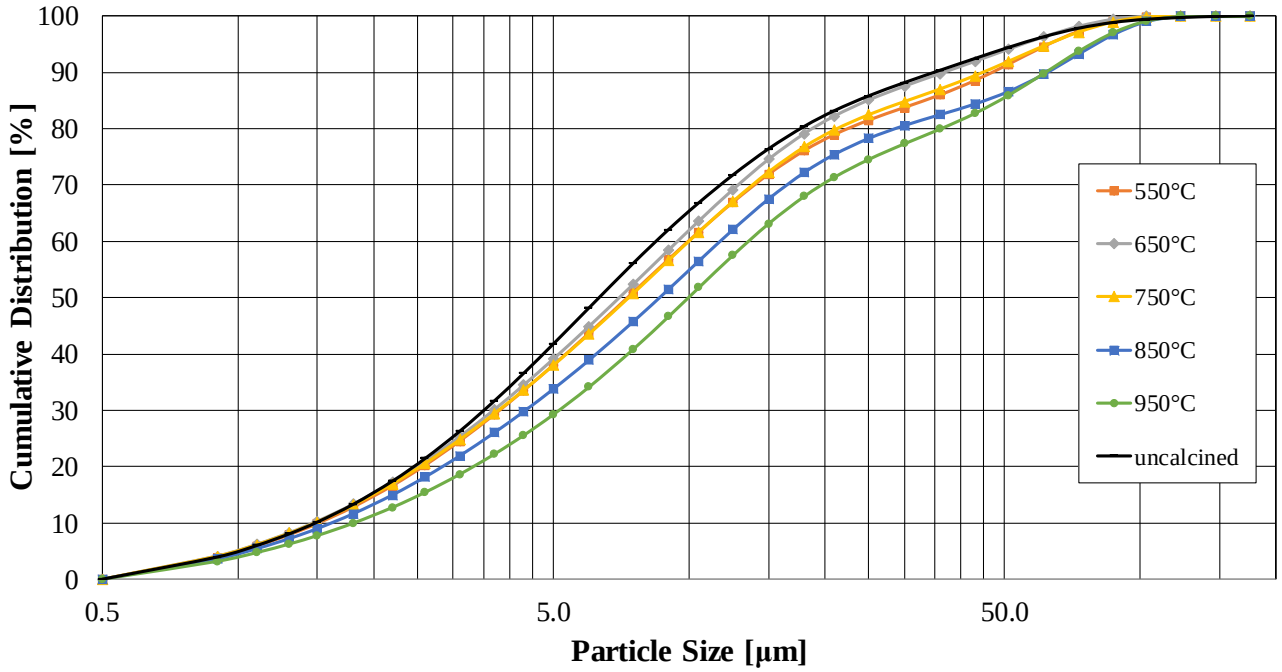

Fig. 3: Particle size distribution of the uncalcined and calcined GWM powders measured by laser granulometry

Element [-]	Content [%]
SiO_2	64.95
Al_2O_3	19.98
Fe_2O_3	9.02
K_2O	3.27
MgO	1.30
TiO_2	0.70
CaO	0.26

Table 2: Chemical composition of the uncalcined GWM particles determined by XRF spectrometry

3.2 Mineralogical composition and thermal analysis

The GWM powders require thermal treatment at high temperatures (calcination) to increase the reactivity of the aluminosilicate materials by dehydration, dehydroxylation and change of the phase composition. This thermal decomposition provides a high-energy, distorted and amorphous raw material, which is favourable for the alkaline dissolution process.

The mineralogy of the uncalcined and the different calcined GWM powders were studied by XRD analysis. The X-ray diffractograms were collected with a D4 ENDEAVOR (Bruker Corporation) powder X-ray diffractometer using Cu Kα radiation at standard scanning parameters. A quantitative analysis was performed following the Rietveld refinement principles (TOPAS, Bruker Corporation) (Paul, 2005). A

quantitative phase analysis was applied instead of a qualitative crystalline phase analysis to quantify the formed amorphous phases due to different calcination temperatures.

Beside the analysis of the mineralogical compositions, this evaluation in combination with the simultaneous thermal analysis (STA) enables to determine an optimum range for duration and temperature level for the thermal treatment of the GWM powder. The sample preparation for XRD analysis was the same as for the previously mentioned XRF analysis.

A quantitative XRD analysis has been carried out for the uncalcined and calcined GWM powders at temperatures of 550°C, 650°C, 750°C, 850°C and 950°C for 1 hour. The calcination time was set to 1 hour based on findings of preliminary tests and suggestions from previous research works (Sabir et al., 2001; Diffo et al., 2015). **Fig. 4** illustrates the reduction of crystalline aluminosilicate minerals with the development of new mineral phases and the rise of amorphous phases regarding the calcination temperatures. First of all, the mineralogy verifies that the aluminosilicate raw material consists of kaolinite and illite as main clay mineral. The dominant phases in all samples are the quartz minerals, followed by clay minerals, muscovite, hematite and the amorphous portions. In addition, from the qualitative analysis of the GWM powder, the presence of low amounts of chlorite was detected, but could not be considered in the quantitative analysis. Higher calcination temperatures lead to transformation of the clay minerals into XRD amorphous phases. In fact, two stages of dehydroxylation can be observed. First, kaolinite is entirely transformed to metakaolinite at temperatures around 600°C, whereas illite becomes amorphous at higher temperatures around 900°C. Furthermore, the content of muscovite is reduced leading to an increase in the content of $KAl_3Si_3O_{11}$, which is a dehydroxilised, crystalline meta-phase of muscovite. Independent on the calcination temperature, the hematite content remains almost constant over all calcination temperatures.

The STA consists of a measurement concept that allows to perform thermogravimetric analysis (TGA) and differential scanning calorimetry (DSC) simultaneously on a single measurement unit. The analysis was carried out from room temperature until 1000°C at a heating rate of 10°C/min in a controlled nitrogen gas atmosphere.

The results of the STA analysis (TG-DSC) are presented in **Fig. 5**. The TG curve shows two mass reduction stages (Total: - 2.62 %) of the investigated sample before 900°C. From about 30°C to 430°C, a first gradual mass loss (- 0.54 %) is observed due to the evaporation of adhesion water of the aluminosilicate minerals and the burnout of organic matters inside the samples. Furthermore, a greater decrease in mass (- 2.09 %) is observed due to the further dehydration of structural water and the dehydroxylation of the crystalline aluminosilicate minerals from 500°C to 975°C until a constant mass state is reached. The DSC curve confirms the process of dehydroxylation of the aluminosilicate matrix, followed by phase transition of the quartz minerals as an endothermic peak is observed at around 575.8°C (quartz inversion). Moreover, the crystallization of the oxides is marked by an exothermic peak at 980°C. The findings of both analysis, mineralogical and thermal, suggest thermal treatment of the GWM powder within the range of 650°C-950°C.

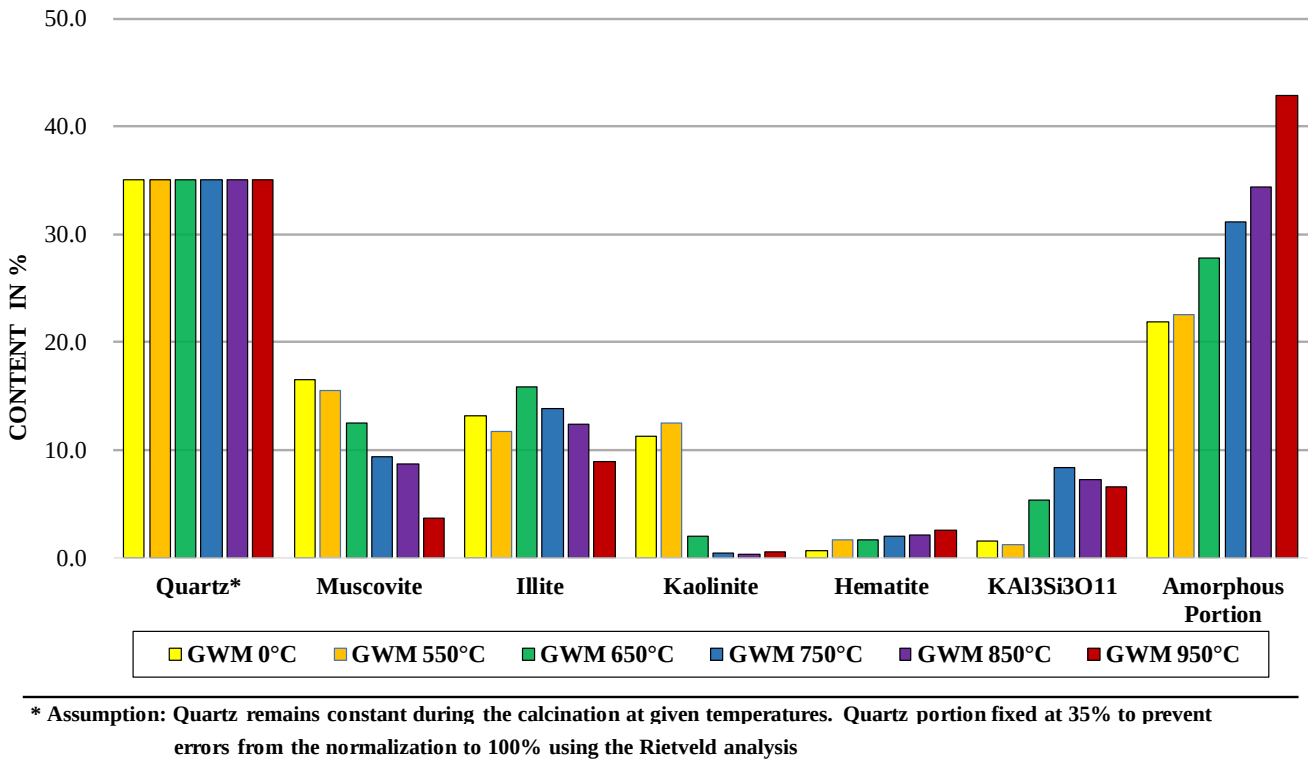

Fig. 4: Results of quantitative X-ray diffraction analysis of the uncalcined and calcined GWM particles at various high temperatures

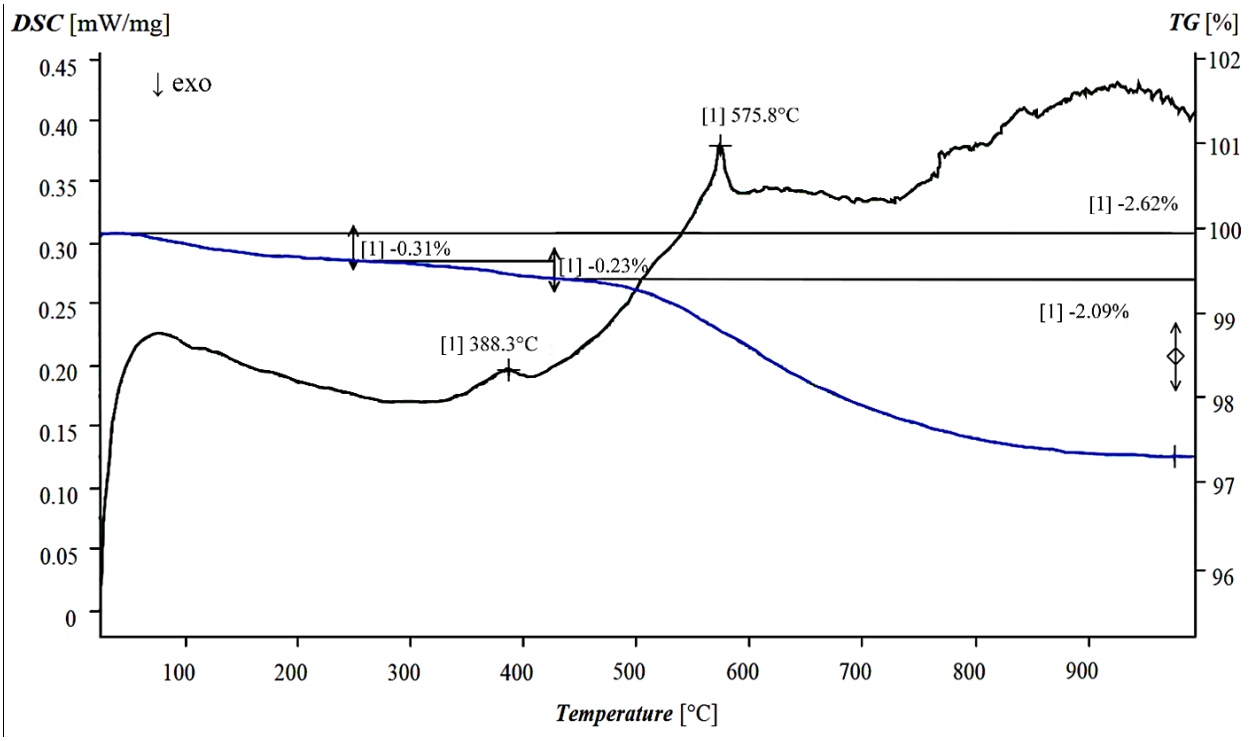

Fig. 5: Results of the STA analysis (TG-DSC) on the GWM powder

3.3 Compressive strength

The compressive strength was measured on three specimens of each mixture after 14 days, 28 days and 56 days using a compression test plant (Toni Technik GmbH) with additional displacement transducers. This measurement unit is optimised for compressive strength tests on prisms (40x40x160 mm^3) according to EN 196 standard. Unhardened specimens after 14 days, mainly specimens including GWM powder calcined at 550°C, were not compressed, as no sign of solidification was observable. **Fig. 6** and **Fig. 7** illustrates the strength development of the binders based on GWM powder calcined at different temperatures without/with sand aggregates. The specimens made with GWM powder calcined at 550°C showed very low compressive strengths and consequently low reactivity. It can be observed that for this GWM powder a higher concentration of the NaOH solution dissolved higher portions of the unreactive aluminosilicate particles and no dense structure could be built. This observation also verifies the predictions from the mineralogical analysis discussed in **section 3.2**. In general, a higher thermal treatment of the GWM powders resulted in a more reactive material, which, in combination with a higher alkaline dissolution degree due to higher molarities of the alkaline solution, exhibited better compressive

strengths. The highest compressive strength of 1.86 MPa was achieved by specimens calcined at 950°C and activated using 14M NaOH solution with sand aggregates. Finally, the results of the compression strength test confirm the dependency of the performance of the GWM-based alkali-activated binder on the calcination temperature of the aluminosilicate prime material, and respectively, its degree of dissolubility in the alkaline medium.

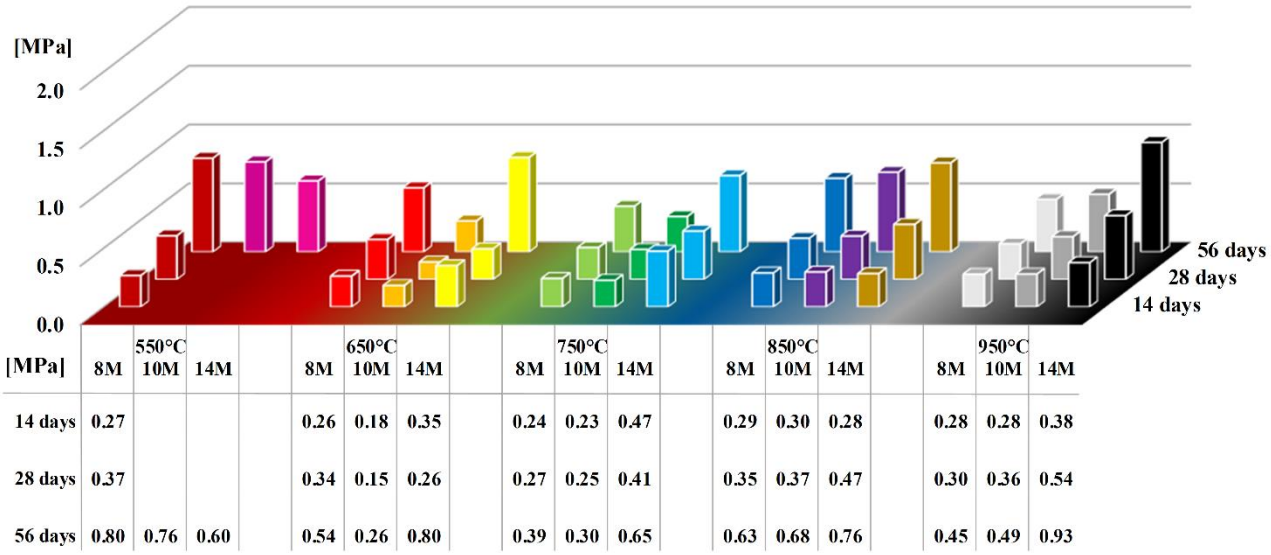

[MPa]	550°C 8M	550°C 10M	550°C 14M	650°C 8M	650°C 10M	650°C 14M	750°C 8M	750°C 10M	750°C 14M	850°C 8M	850°C 10M	850°C 14M	950°C 8M	950°C 10M	950°C 14M
14 days	0.27			0.26	0.18	0.35	0.24	0.23	0.47	0.29	0.30	0.28	0.28	0.28	0.38
28 days	0.37			0.34	0.15	0.26	0.27	0.25	0.41	0.35	0.37	0.47	0.30	0.36	0.54
56 days	0.80	0.76	0.60	0.54	0.26	0.80	0.39	0.30	0.65	0.63	0.68	0.76	0.45	0.49	0.93

Fig. 6: Strength development of GWM-based binders without sand aggregates for varying calcination temperatures, varying concentrations of NaOH solutions and concrete ages

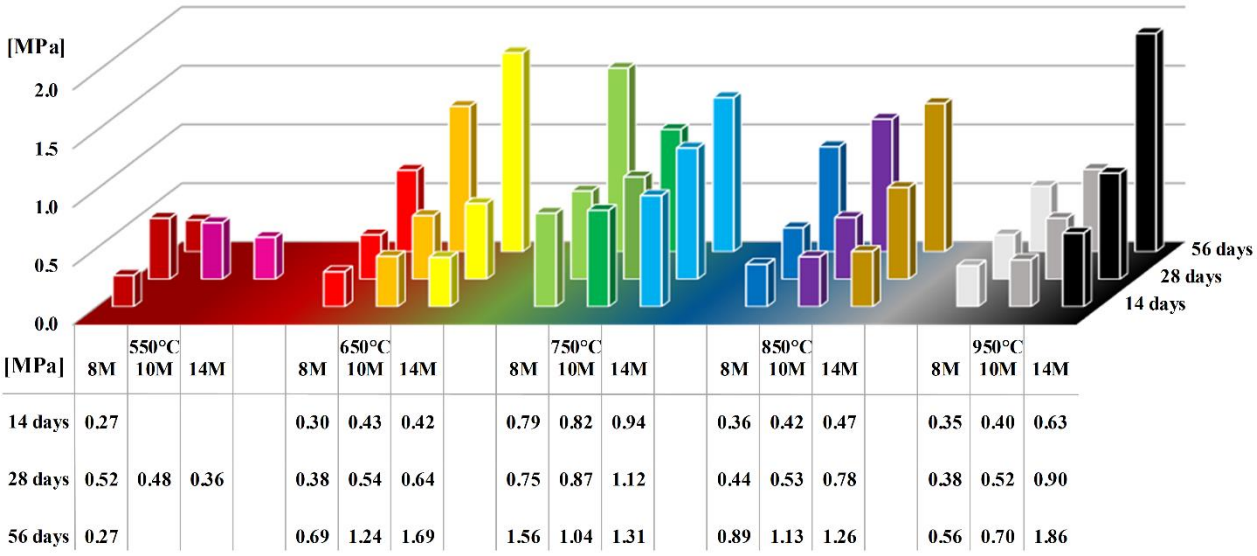

[MPa]	550°C 8M	550°C 10M	550°C 14M	650°C 8M	650°C 10M	650°C 14M	750°C 8M	750°C 10M	750°C 14M	850°C 8M	850°C 10M	850°C 14M	950°C 8M	950°C 10M	950°C 14M
14 days	0.27			0.30	0.43	0.42	0.79	0.82	0.94	0.36	0.42	0.47	0.35	0.40	0.63
28 days	0.52	0.48	0.36	0.38	0.54	0.64	0.75	0.87	1.12	0.44	0.53	0.78	0.38	0.52	0.90
56 days	0.27			0.69	1.24	1.69	1.56	1.04	1.31	0.89	1.13	1.26	0.56	0.70	1.86

Fig. 7: Strength development of GWM-based binders with sand aggregates for varying calcination temperatures, varying concentrations of NaOH solutions and concrete ages

3.4 Analysis of the microstructure

The microstructure of all binders was analysed by SEM using LEO 440 REM, which is a compact and high performing SEM unit that enables high quality observations of structure surfaces down to 5 nm realised by detection of secondary backscattered electrons from a high-energy beam of primary electrons in a raster scan pattern.

The images of the microstructure of selected alkali-activated binders (**Fig. 8**) were obtained by performing SEM on small fractions of the compressed specimens. **Fig. 8.a-b** show the microstructure of the binders realised based on GWM powders calcined at 550°C. The binder in **Fig. 8.a** shows a compact composition, which envelops the quartz particle, whereas comparatively, the binder in **Fig. 8.b** shows a more porous composition and the coverage of the quartz particle is loose and weak. As already supposed in the mineralogical analysis (**section 3.2**) and supported by the compressive strength test (**section 3.3**), these binders (using calcined GWM at 550°C) possess highly disintegrated, low reactive aluminosilicate constituents formed by the dissolution in higher alkaline solutions, which lead to a weaker binder framework. In comparison with these binders (**Fig. 8.c-f**), binders realised on the basis of GWM powders with higher thermal treatment show larger flaky, plate-like meta-clay minerals and needle-like mineral formations which provide larger reactive surfaces for the development of a compact microstructure. Finally, **Fig. 8.g-h** presents the morphology of binders subjected to higher alkalinity and based on GWM powders calcined at higher temperatures. These microstructures present a well-formed morphology of the constituents resulting in a dense and compact matrix comprising flaky meta-clays, needle-like crystal formations and amorphous material.

The GWM's fineness with its chemical and mineralogical composition provided an auspicious base to assess its suitability for the synthesis of an alkali-activated binder. Even though the developed microstructures showed a well-developed binder framework, the achieved compressive strengths were small. These results suggest that GWM without any further additives or processing is not recommended as a precursor for alkaline activation. This outcome can be explained by the low silica content in the binder compared to the alumina content, respectively, the lower portion of reactive clay minerals

compared to the dominant quartz content from a mineralogical point of view. Thereby, the calcined materials comprise lower contents of reactive meta-clays to take part in the reactions. In comparison, hardened mixtures based on raw materials with higher contents of kaolinite can achieve compressive strengths above 38.5 MPa (Kong et al., 2007) or 48.8 MPa (Tchakoute et al., 2015) depending on the characteristics of the raw materials and the applied alkaline solution.

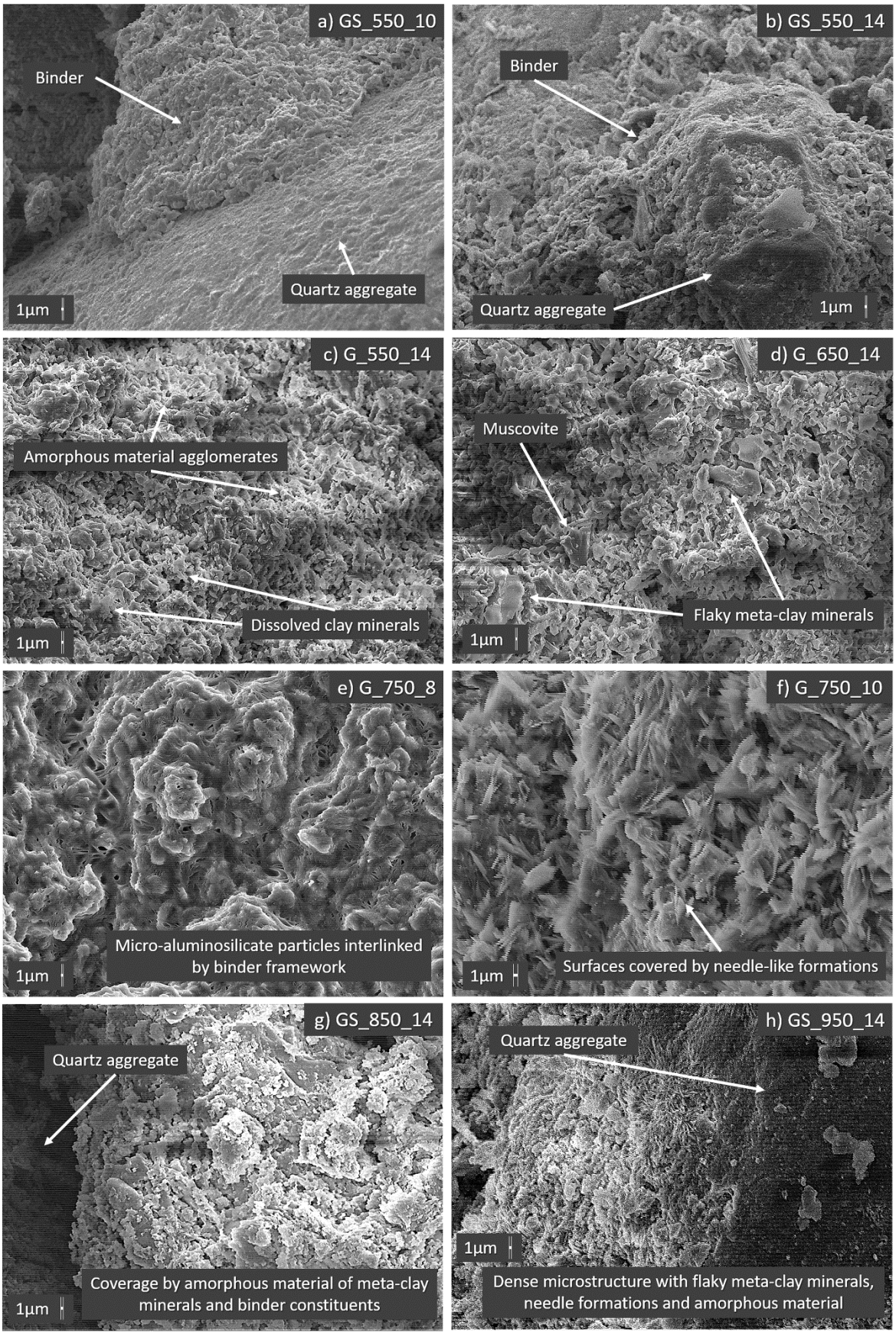

Fig. 8: Scanning electron micrographs of selected specimens showing the morphology of the constituents of the alkali-activated binders in the micron range (image scale of 1µm; magnification up to 3600 x)

4 CONCLUSION

This study presents the results of investigations carried out on alkali-activated binder using calcined GWM as prime material. The key findings from different material characterisation methods and experimental tests on specimens are summarized below:

(1) The GWM powder consists of quartz with a moderate content of clay minerals (illite and kaolinite), muscovite, and a small portion of hematite and chlorite.

(2) The XRD analysis reveals the reduction of crystalline aluminosilicate minerals with the development of new mineral phases and the rise of amorphous phases with increasing calcination temperatures from 550°C to 950°C. During calcination, two stages of dehydroxylation were observed: The complete conversion of kaolinite to metakaolinite at around 600°C and illite becomes amorphous at higher temperatures above 900°C.

(3) The results of the STA analysis confirm the process of dehydroxylation of the aluminosilicate matrix, followed by quartz inversion (endothermic peak at 575.8°C). Moreover, the crystallization of the oxides is marked by an exothermic peak at 980°C.

(4) The highest 56-day compressive strength of the binders was 1.86 MPa and occurred for the mixture using GWM powder calcined at 950°C with a 14M NaOH solution and mixed with sand aggregates.

(5) The microstructure presents a well-formed morphology of the constituents resulting in a dense and compact matrix comprising flaky meta-clays, needle-like mineral formations and amorphous material.

Further studies are required to foster greater understanding of the reactivity and reaction mechanisms of binders based on this raw material. In addition, it is necessary to investigate on the activation effectiveness of different types of alkalis like potassium hydroxide, water glass and others. Finally, the understanding of complex solid phases is essential to analyse their effects on the long-term behaviour of alkali-activated binders.

5 ACKNOWLEDGEMENTS

The authors gratefully acknowledge Carrières Feidt S.A. for the supply of the gavel wash mud (GWM), Cimalux S.A. with its partner institution Wilhelm Dyckerhoff Institut (WDI) for their contributions in the material characterisation and Contern S.A. for the supply of required materials and tools.

BIBLIOGRAPHY

Aguirre-Guerrero, A. M., Robayo-Salazar, R. A., & de Gutiérrez, R. M. (2017). A novel geopolymer application: Coatings to protect reinforced concrete against corrosion. Applied Clay Science, 135, 437-446.

Aramide, F. O., 2015. Effects of sintering temperature on the phase developments and mechanical properties ifon clay. Leonardo Journal of Sciences, 26, 67-82.

Balek, V., Murat, M., 1996. The emanation thermal analysis of kaolinite clay minerals. Thermochimica Acta, 282, 385-397.

Bignozzi, M. C., Manzi, S., Lancellotti, I., Kamseu, E., Barbieri, L., Leonelli, C., 2013. Mix-design and characterization of alkali activated materials based on metakaolin and ladle slag. Applied Clay Science, 73, 78-85.

Brunauer, S., Emmett, P. H., Teller, E., 1938. Adsorption of gases in multimolecular layers. Journal of the American chemical society, 60 (2), 309-319.

Buchwald, A., Hohmann, M., Posern, K., Brendler, E., 2009a. The suitability of thermally activated illite/smectite clay as raw material for geopolymer binders. Applied Clay Science, 46 (3), 300-304.

Buchwald, A., Vicent, M., Kriegel, R., Kaps, C., Monzó, M., Barba, A., 2009b. Geopolymeric binders with different fine fillers-phase transformations at high temperatures. Applied Clay Science, 46 (2), 190-195.

Chen, J. H., Huang, J. S., Chang, Y. W., 2009. A preliminary study of reservoir sludge as a raw material of inorganic polymers. Construction and Building Materials, 23 (10), 3264-3269.

Cowley, J. M., 1995. Diffraction physics. Elsevier.

Davidovits, J., 1979. Synthesis of New High-Temperature Geo-Polymers for Reinforced Plastics/Composites, SPE PACTFC 79, Society of Plastic Engineers, Brookfield Center, USA, pp. 151–154.

Davidovits, J., Comrie, D. C., Paterson, J. H., Ritcey, D. J., 1990. Geopolymeric concretes for environmental protection. Concrete International, 12 (7), 30-40.

Davidovits, J., 1994. Properties of geopolymer cements. First international conference on alkaline cements and concretes, Vol. 1, 131-149.

Davidovits, J., Sawyer, J. L., 1985. U.S. Patent No. 4,509,985, EP No.0153097.

Diffo, B. K., Elimbi, A., Cyr, M., Manga, J. D., Kouamo, H. T., 2015. Effect of the rate of calcination of kaolin on the properties of metakaolin-based geopolymers. Journal of Asian Ceramic Societies, 3 (1), 130-138.

Escalante-García, J. I., Gorokhovsky, A. V., Mendoza, G., Fuentes, A. F., 2003. Effect of geothermal waste on strength and microstructure of alkali-activated slag cement mortars. Cement and concrete research, 33 (10), 1567-1574.

Ferone, C., Colangelo, F., Cioffi, R., Montagnaro, F., Santoro, L., 2013. Use of reservoir clay sediments as raw materials for geopolymer binders. Advances in Applied Ceramics, 112 (4), 184-189.

Friedlingstein, P., Andrew, R. M., Rogelj, J., Peters, G. P., Canadell, J. G., Knutti, R., Luderer, G., Raupach, M. R., Schaeffer, M., van Vuuren, D. P., Le Quéré, C., 2014. Persistent growth of CO_2 emissions and implications for reaching climate targets. Nature geoscience, 7 (10), 709-715.

García-Gusano, D., Cabal, H., Lechón, Y., 2015. Long-term behaviour of CO_2 emissions from cement production in Spain: scenario analysis using an energy optimisation model. Journal of Cleaner Production, 99, 101-111.

Gartner, E., Hirao, H., 2015. A review of alternative approaches to the reduction of CO_2 emissions associated with the manufacture of the binder phase in concrete. Cement and Concrete research, 78, 126-142.

Glukhovsky, V. D., 1959. Soil silicates. Gostroiizdat Publish. Kiev, USSR.

385 Glukhovsky, V. D., Rostovskaja, G. S., Rumyna, G. V., 1980. High strength slag-alkaline cements. In
386 Proceedings of the 7th international congress on the chemistry of cement, Paris, 164-168.
387 Heitsmann, R. F., Fitzgerald, M., Sawyer, J. L., 1987. U.S. Patent No.4.643.137.
388 Kong, D. L., Sanjayan, J. G., & Sagoe-Crentsil, K., 2007. Comparative performance of geopolymers made
389 with metakaolin and fly ash after exposure to elevated temperatures. Cement and Concrete Research,
390 37 (12), 1583-1589.
391 Le Saoût, G., Kocaba, V., Scrivener, K., 2011. Application of the Rietveld method to the analysis of
392 anhydrous cement. Cement and concrete research, 41 (2), 133-148.
393 Liu, Z., Guan, D., Wei, W., Davis, S. J., Ciais, P., Bai, J., ..., Andres, R. J., 2015. Reduced carbon emission
394 estimates from fossil fuel combustion and cement production in China. Nature, 524 (7565), 335-338.
395 Lucius, M., 1948. Erläuterungen zur geologischen Karte Luxemburgs–Das Gutland. Publications du
396 Service Géologique de Luxembourg, Luxembourg.
397 Lucius, M., 1950. Geologie Luxemburgs: Erläuterungen zu der geologischen Spezialkarte Luxemburgs.
398 Das Oesling.
399 Messina, F., Ferone, C., Molino, A., Roviello, G., Colangelo, F., Molino, B., Cioffi, R., 2017. Synergistic
400 recycling of calcined clayey sediments and water potabilization sludge as geopolymer precursors:
401 Upscaling from binders to precast paving cement-free bricks. Construction and Building Materials,
402 133, 14-26.
403 Molino, B., De Vincenzo, A., Ferone, C., Messina, F., Colangelo, F., Cioffi, R., 2014. Recycling of clay
404 sediments for geopolymer binder production. A new perspective for reservoir management in the
405 framework of Italian legislation: The Occhito reservoir case study. Materials, 7 (8), 5603-5616.
406 Myers, R. J., Bernal, S. A., Provis, J. L., 2017. Phase diagrams for alkali-activated slag binders. Cement
407 and Concrete Research, 95, 30-38.
408 Pacheco-Torgal, F., Castro-Gomes, J., Jalali, S., 2007. Investigations about the effect of aggregates on
409 strength and microstructure of geopolymeric mine waste mud binders. Cement and Concrete
410 Research, 37 (6), 933-941.

411 Pacheco-Torgal, F., Abdollahnejad, Z., Camões, A. F., Jamshidi, M., Ding, Y., 2012. Durability of alkali-
412 activated binders: a clear advantage over Portland cement or an unproven issue?. Construction and
413 Building Materials, 30, 400-405.
414 Paul, M., 2005. Application of the Rietveld method in the cement industry. Proceed. Microstructure
415 Analysis in Materials Science, 1-3.
416 Phair, J. W., Van Deventer, J. S. J., 2001. Effect of silicate activator pH on the leaching and material
417 characteristics of waste-based inorganic polymers. Minerals Engineering, 14 (3), 289-304.
418 Poowancum, A., Nimwinya, E., Horpibulsuk, S., 2015. Development of Room Temperature Curing
419 Geopolymer from Calcined Water-Treatment-Sludge and Rice Husk Ash. Calcined Clays for
420 Sustainable Concrete, 291-297.
421 Provis, J. L., Van Deventer, J. S. J. (Eds.), 2009. Geopolymers: structures, processing, properties and
422 industrial applications. Elsevier.
423 Provis, J. L., 2014. Geopolymers and other alkali activated materials: why, how, and what?. Materials
424 and Structures, 47(1-2), 11-25.
425 Provis, J. L., Palomo, A., Shi, C., 2015. Advances in understanding alkali-activated materials. Cement
426 and Concrete Research, 78, 110-125.
427 Provis, J. L., 2017. Alkali-activated materials. Cement and Concrete Research.
428 Roy, A., Schilling, P. J., Eaton, H. C., Malone, P. G., Brabston, W. N., Wakeley, L. D., 1992. Activation
429 of ground blast-furnace slag by alkali-metal and alkaline-Earth hydroxides. Journal of the American
430 Ceramic Society, 75 (12), 3233-3240.
431 Sabir, B. B., Wild, S., Bai, J., 2001. Metakaolin and calcined clays as pozzolans for concrete: a review.
432 Cement and Concrete Composites, 23 (6), 441-454.
433 Salas, D. A., Ramirez, A. D., Rodríguez, C. R., Petroche, D. M., Boero, A. J., & Duque-Rivera, J., 2016.
434 Environmntal impacts, life cycle assessment and potential improvement measures for cement
435 production: a literature review. Journal of Cleaner Production, 113, 114-122.

436 Shi, C., Wu, X., & Tang, M., 1991. Hydration of alkali-slag cements at 150°C. Cement and Concrete
437 Research, 21 (1), 91-100.
438 Shi, C., Jiménez, A. F., & Palomo, A., 2011. New cements for the 21st century: the pursuit of an
439 alternative to Portland cement. Cement and concrete research, 41 (7), 750-763.
440 Sun, Z., Cui, H., An, H., Tao, D., Xu, Y., Zhai, J., Li, Q., 2013. Synthesis and thermal behavior of
441 geopolymer-type material from waste ceramic. Construction and Building Materials, 49, 281-287.
442 Tchakoute, H. K., Rüscher, C. H., Djobo, J. N. Y., Kenne, B. B. D., Njopwouo, D., 2015. Influence of
443 gibbsite and quartz in kaolin on the properties of metakaolin-based geopolymer cements. Applied
444 Clay Science, 107, 188-194.
445 Wagner, J.-F., 1989. Paläogeographische Entwicklung der triadischen Randfazies Luxemburgs. Z. dt.
446 geol. Ges., (140), Hannover, 311-331.
447 Wang, S. D., Scrivener, K. L., Pratt, P. L., 1994. Factors affecting the strength of alkali-activated slag.
448 Cement and concrete research, 24 (6), 1033-1043.
449 Wang, S. D., Scrivener, K. L., 1995. Hydration products of alkali activated slag cement. Cement and
450 Concrete Research, 25 (3), 561-571.
451 Wang, S. D., Pu, X. C., Scrivener, K. L., Pratt, P. L., 1995. Alkali-activated slag cement and concrete: a
452 review of properties and problems. Advances in cement research, 7 (27), 93-102.
453 Wianglor, K., Sinthupinyo, S., Piyaworapaiboon, M., Chaipanich, A., 2017. Effect of alkali-activated
454 metakaolin cement on compressive strength of mortars. Applied Clay Science, 141, 272-279.
455 Yunsheng, Z., Wei, S., Zongjin, L., 2010. Composition design and microstructural characterization of
456 calcined kaolin-based geopolymer cement; Applied Clay Science, 47 (3), 271-275.